ARR No. 3F24

NATIONAL ADVISORY COMMITTEE FOR AERONAUTICS

WARTIME REPORT

ORIGINALLY ISSUED
June 1943 as
Advance Restricted Report 3F24

WIND-TUNNEL VIBRATION TESTS OF A FOUR-BLADE SINGLE-ROTATING PUSHER PROPELLER

By Mason F. Miller

Langley Memorial Aeronautical Laboratory
Langley Field, Va.

NACA

WASHINGTON

NATIONAL ADVISORY COMMITTEE FOR AERONAUTICS

ADVANCE RESTRICTED REPORT

WIND-TUNNEL VIBRATION TESTS OF A FOUR-BLADE SINGLE-ROTATING PUSHER PROPELLER

By Mason F. Miller

SUMMARY

Vibration tests of a four-blade single-rotating propeller operating in a simulated pusher condition were performed because the combination of wake and downwash behind a wing was expected to provide serious excitation for reactionless vibrations of propellers with four or more blades. The tests were conducted in the LMAL 16-foot high-speed tunnel with a wing mounted at thrust-axis level ahead of the propeller; the blade sections at three-fourths the propeller radius operated at approximately twice their chords behind the trailing edge of the tapered wing at their closest position. Measurements of propellor vibratory stress were made for various airspeeds, engine speeds, and engine powers.

The wake behind the wing supplied serious excitation for an edgewise reactionless vibration of the propeller at a frequency of twice the propeller speed; the resulting vibratory stress increased considerably with airspeed but was practically independent of engine brake mean effective pressure for constant airspeeds. The effect of downwash upon the reactionless vibration was very small; changing the angle of attack of the wing from 0° to 3.9° produced no detectable increase of downwash excitation and little increase of wake excitation. A simulated full-span split flap on the lower surface of the wing greatly increased the vibratory stress and prohibited the running of tests over the stress peak at airspeeds higher than 140 miles per hour.

No flatwise reactionless vibration was detected, probably because the airspeeds were low for most of the critical engine speeds and because the harmonic components of wake excitation were small.

INTRODUCTION

The operation of a single-rotating propeller with four or more blades behind the wing has created some concern because of the expectation that the combination of wake and downwash might supply serious excitation for a reactionless type of vibration. Because reactionless vibrations of a single-rotating propeller may occur at all frequencies other than 1, kB, and kB ±1 times the propeller speed where k is any integer and B is the number of blades, it is observed that the propeller must have more than three blades to vibrate in a reactionless manner (reference 1). A propeller vibration is reactionless if the vibratory motions of the blades are such that the vibratory bending moments and the vibratory forces of the several blades cancel each other at the propeller shaft; consequently, reactionless vibrations occur only with aerodynamic excitation and are not possessed of engine damping. It was believed that with no engine damping the vibratory stresses caused by the wake and the downwash behind a wing could be unsatisfactorily high, inasmuch as the vibratory stresses would be limited only by aerodynamic damping, by hysteresis damping of the propeller blades, and by damping produced by motion of the blade shanks in their hub sockets.

Tests were conducted in the LMAL 16-foot high-speed tunnel with a wing mounted at thrust-axis level ahead of a four-blade single-rotating propeller. Measurements of propeller vibratory stress were made for various airspeeds, engine powers, and conditions of the wing for the complete engine-speed range. Most of the testing was done, however, within the limited range of engine speed for which a prominent reactionless vibration occurred.

Members of the staff of Hamilton Standard Propellers, Division of United Aircraft Corporation, collaborated in conducting the tests and analyzing the records.

APPARATUS AND METHODS

The single-rotating propeller tested is described as follows:

Type	Hamilton Standard hydromatic
Material	Aluminum alloy
Number of blades	Four
Diameter	12 feet 0 inches
Blade design	6487-12
Hub design	24D50

The propeller was driven by a Pratt & Whitney R-2800 engine geared 16:9 and mounted on rubber mounts in a full-scale stub-wing nacelle. The engine-propeller-nacelle combination is shown in figure 1.

The pusher condition was simulated by mounting a wing at thrust-axis level ahead of the four-blade propeller. The wing, which has an NACA low-drag airfoil section, was inverted merely because of convenience, this way of mounting having been desirable for conducting the vibration tests reported in reference 2. Figure 1 shows the wing mounted ahead of the propeller to simulate the pusher condition. The dimensions of the wing and the location of the wing with respect to the propeller for the wing set at an angle of attack α of 0° are shown in figure 2. The wing was located in such a way that the blade sections at three-fourths the propeller radius operated at approximately twice their chords behind the trailing edge of the tapered wing. The simulated split flap used for one of the tests is shown in figure 2. In order that the simulated flap would be attached to the rear spar of the wing, it was somewhat forward of the usual flap position.

Oscillograph records of propeller vibratory strain were obtained by a method fully described in reference 2.

Electrical strain gages were mounted longitudinally on all the blades at the shanks and near the tips. The gages were mounted on the cambered — that is, the front — sides of the blades (fig. 3). Because the maximum stress of a blade surface for a given propeller radius is at maximum blade thickness for a flatwise vibration, the tip gages were mounted to measure stresses at maximum blade thicknesses. Some gages were mounted on the wing.

The strain gages on the propeller were connected to a slip-ring device, which in turn was connected to voltage amplifiers. The strain-gage resistances varied with the strains to produce fluctuating voltages the alternating components of which were applied to the amplifiers.

The gages were calibrated in such a way that there was a known relationship between the alternating voltages and the strain variations.

The alternating-voltage outputs of the amplifiers were applied to oscillograph elements of a recording oscillograph, and strain variations were recorded on photographic paper. There were 12 amplifiers and 12 oscillograph elements; one of the channels was used for recording a timing wave on the photographic paper. The timing wave consisted in periodic impulses occurring each time a given cylinder fired. These impulse records were obtained by proper connection from a spark-plug lead to an oscillograph element. The purpose of having a timing wave representing engine speed is to express the frequencies of vibration in terms of either engine speed or propeller speed, in order that the cause of the vibration can be determined. A direct record of propeller speed would have been just as suitable. (See reference 2.)

All the amplifiers were calibrated simultaneously at intervals during the test by applying a known alternating voltage to their input terminals. The amplitudes of the resulting oscillograph traces were measured after the tests, and a definite relationship between oscillograph amplitudes and amplifier input voltages was thereby obtained. Each inch of amplitude on the photographic paper therefore represented a known amplitude of strain on a propeller blade. Stress values were determined by multiplying strain values by the modulus of elasticity for aluminum.

The static natural frequencies of reactionless propeller vibrations with Hamilton Standard 6487-12 blades were predetermined by measurement and are shown in the following table:

Mode	Frequency (cps)
Flatwise	16.7
	70.2
	137.8
	187.5
	230.5
Edgewise	45.8

The four-blade propeller, resting on its hub which was unrestrained, was excited at one of the blade tips with an electrical exciter of variable frequency. It was considered not necessary to restrain the hub because, for a reactionless vibration, the vibratory bending moments and vibratory forces of the four blades cancel each other at the hub. From a low frequency, the exciter frequency was gradually increased; when the various reactionless vibrations appeared, the frequencies were accurately determined. Oscillograph records of strain were taken, using electrical strain gages for pickups; the frequencies of strain variation appearing on these records were determined accurately by comparing them with the traces produced by an accurately calibrated, electrically excited tuning fork. Frequencies for the first five flatwise modes and the first edgewise mode were determined. Because the present report deals principally with reactionless vibrations, the method of determining static natural frequencies of nonreactionless vibrations is not discussed herein. A more complete discussion of the methods of measuring static natural frequencies of a propeller is given in reference 2.

A propeller vibration is termed flatwise if the vibratory motions of the blade sections are primarily perpendicular to the blade chords; whereas an edgewise propeller vibration is one with the vibratory motions of the blade sections primarily along the blade chords. Some flatwise motion generally exists near the blade tips during edgewise resonance because of the coupling supplied by the blade twist.

Centrifugal correction factors were applied to the static natural frequencies of reactionless vibration in accordance with the accepted formula, which is explained in reference 3,

$$f^2 = f_0^2 + Kn^2 \qquad (1)$$

where

f natural frequency at a given propeller speed

f_0 static natural frequency

n propeller speed

and

K a constant for a given mode of a given propeller

The method of predicting engine speeds for reactionless vibrations of frequencies 2n and 6n is shown in figure 4. The values of K used for figure 4 are as follows:

First flatwise mode	1.7
Second flatwise mode	5.6
First edgewise mode	1.12

The critical engine speeds are those at which the straight lines intersect the lines representing natural frequencies. Only the first and the second flatwise modes and the first edgewise mode are considered for figure 4 because, within the engine operating speeds, the straight lines representing frequencies of 2n and 6n do not intersect the natural-frequency lines for the higher modes. The reactionless vibration having a frequency of 2n is of most importance and the reactionless vibration of frequency 6n is also of interest. Excitations having frequencies higher than 6n were expected to be negligible.

The test conditions are given in the following table:

Engine bmep (lb/sq in.)	Airspeed (mph)	Engine speed (rpm)
Angle of attack, 0°		
100	15 to 280	900 to 2850
150	100 to 280	1250 to 2850
200	100 to 280	1250 to 2860
Angle of attack, 3.9°		
100	100 to 185	2400 to 2850
150	100 to 185	2400 to 2850
200	100 to 185	2400 to 2850
Angle of attack, 0°; simulated split flap on wing		
100	100 to 185	2400 to 2850
150	100 to 185	2400 to 2850
200	100 to 185	2400 to 2850

GENERAL DISCUSSION OF PROPELLER VIBRATIONS CAUSED BY A WING AHEAD OF THE PROPELLER

Sizable excitation forces for reactionless propeller vibrations are expected if the propeller operates in the wake and downwash region behind a wing. Although nonreactionless vibrations having other excitations are also important, they are outside the scope of the present report.

In accordance with the result of an analysis showing that reactionless vibrations can occur for all frequencies other than 1, kB, and kB $\pm$ 1 times the propeller speed, a propeller must have more than three blades to vibrate in a reactionless manner, and a reactionless vibration of a four-blade propeller can occur for frequencies of 2n, 6n, 10n, 14n . . . (reference 1). It may be noted that a reactionless vibration can occur at a frequency of 2n for propellers with four or more blades.

The wake behind a wing may result in a serious reactionless vibration of a propeller with four or more blades if the frequency of excitation 2n is equal to a natural frequency for a reactionless vibration. Each blade of the propeller passes through two low-velocity regions per revolution. The periodic change of forward velocity with respect to each blade causes a periodic change of angle of attack of each blade. Periodic forces therefore act upon the blades to produce a propeller vibration at a frequency of 2n. The effect of a change of forward velocity acting upon the propeller blades is shown in figure 5. The greater force occurs for the lower forward velocity because of the greater angle of attack. The decrease in magnitude of resultant velocity V_R, however, slightly offsets the effect of the change of the angle of attack. Typical total-pressure and static-pressure variations in the wake region are shown in figure 6.

The excitation provided by the wake is not sinusoidal, and excitations at frequencies that are harmonics of 2n therefore exist. These harmonic components, however, are smaller than the fundamental component. The excitation having a frequency of 4n will not excite a reactionless vibration of a four-blade propeller. Although an excitation having a frequency of 6n can produce a reactionless

vibration, the third harmonic component of wake excitation is expected to be quite small and to give little trouble. Higher harmonics of wake excitation are expected to be negligible.

A reactionless vibration having a frequency of 6n can be a first, a second, or a higher mode, depending upon the propeller speed. The highest mode that can be obtained with this frequency of 6n depends upon the upper limit of propeller speed, the natural frequencies of the modes, and the increase of natural frequencies of the modes with propeller speed. (See references 2 and 3.) For modes of vibration higher than the first mode, the vibratory velocity of some parts of the blade is 180° out of phase with that at other parts of the blade (see fig. 7); and, with the excitation acting in the same sence over the entire blade length, some parts of the blade absorb energy from the excitation, while the remaining parts dissipate energy. If a reactionless vibration of frequency 6n appeared at a relatively high propeller speed, it would be one of the higher modes and therefore subject to the cancelation effect. The cancelation effect is somewhat decreased, however, because an excitation acting near a blade tip is more effective than the same excitation acting near the blade shank.

The presence of downwash behind a wing is expected to supply excitation for a propeller vibration at a frequency of 1n, as shown in figure 8. The downward component of velocity in the plane of the propeller disk increases the angle of attack of a propeller blade during one-half revolution of the propeller and decreases this angle during the remaining one-half revolution. This periodic change of angle of attack of the blades causes periodic forces to act on the blades and therefore results in a propeller vibration at a frequency of 1n. Also, the resultant velocity V_R of the air with respect to the blades is variable with the same frequency as the angle of attack and aids the periodic change of angle of attack to produce the vibration. The vibration at a frequency of 1n excited by the downwash is not reactionless but, if it occurs simultaneously with the reactionless vibration, is expected to increase the seriousness of the reactionless vibration excited by the wake.

Increasing the angle of attack of a wing causes an increase of downwash angle and, as a result, a vibration excited by downwash would be expected to become more pro-

nounced. Although the wake behind a wing follows the downwash, the change of magnitude and shape of a wake profile is small for a change of angle of attack less than about 5°. (See reference 4.) A relatively small change of wing angle of attack is therefore expected to produce little change of a propeller vibration excited by the wake.

The use of a split flap on a wing is expected to broaden and strengthen the wake (reference 4) and thereby considerably increase the propeller vibratory stress occurring at a frequency of 2n. A split flap on the lower surface of a wing also directs the air downward behind the wing and is expected to increase the excitation at a frequency of 1n.

For constant airspeed and propeller speed, the propeller vibrations excited by the wake and the downwash behind a wing would be expected to be less affected by the engine brake mean effective pressure than those propeller vibrations excited by the engine.

The trailing edge of a wing may possibly vibrate because of aerodynamic excitation supplied by a propeller operating close behind it, if its natural frequency is equal to the frequency of excitation (reference 2). The frequency of importance is Bn; each blade passes the closer part of the trailing edge once per propeller revolution.

DISCUSSION OF RESULTS

The results of the present test are presented in figures 9 to 12. The stress peaks are labeled with vibration frequencies in terms of propeller speed n and engine speed N — for example, 2n and $4\frac{1}{2}$N. The stress peaks of the curves representing total vibratory stress have more than one frequency component, and the frequency components are given in order of importance. Some of the stress curves are given only for a frequency of 2n; these stresses were measured with a wave analyzer.

A prominent propeller vibration having a frequency of 2n appeared at an engine speed between 2780 rpm and 2840 rpm. (See fig. 9.) This vibration was evidently edgewise, inasmuch as the first mode of edgewise vibration at a frequency of 2n was predicted for an engine speed of 2880 rpm (fig. 4). The engine-speed prediction was

somewhat high but is considered good, any prediction within 50 rpm being satisfactory for test purposes. The curves of figure 9 are plotted for the leading-edge position of the shank for two reasons: (1) For an edgewise vibration, the stresses at the shank are maximum at the leading edge and 180° around the shank from the leading edge, as discussed in reference 2 (the leading-edge position is in line with the leading edge at approximately the 42-in. station of the blade); and (2) For a first mode of vibration, the maximum stress along a blade is near the propeller hub because stress depends upon c/ρ, where c is the perpendicular distance from the neutral axis to the extreme fiber and ρ is the radius of curvature of the neutral axis.

The effect of airspeed upon the vibratory stress for the edgewise vibration appearing at an engine speed of 2820 rpm is shown in figure 9. These curves demonstrate that the vibratory stress increased with airspeed. Part of the total vibratory stress was produced by engine excitation, as evidenced by the frequencies $4\frac{1}{2}N$, $1N$, and $1\frac{7}{16}N$.

The effect of engine brake mean effective pressure upon the vibratory stress is shown in figure 9. The vibratory stresses having frequencies of $2n$ change only slightly with brake mean effective pressure for a given airspeed; the very slight variation can be due to experimental error. The vibratory stress of frequency $2n$ would be expected to be practically independent of brake mean effective pressure, as previously discussed; however, if the total vibratory stress is composed of some engine-excited components, some engine damping exists that may vary with brake mean effective pressure to produce such slight variations of stress as found in figure 9. At first glance, the bottom curves seem to vary considerably with engine brake mean effective pressure, but it must be noticed that the curves are plotted for slightly different airspeeds.

The downwash behind the wing should provide excitation at a frequency of $1n$. With a wing angle of attack of 0°, traces of vibrations having a frequency of $1n$ were found for an airspeed of 280 miles per hour, but no indication of the frequency $1n$ appeared at the lower airspeeds. (See fig. 9.) The effect of downwash upon the total vibratory stress at the engine speed of 2820 rpm is small, probably because a frequency of $1n$ at this

engine speed is not a natural frequency of propeller vibration and because the downwash is limited in a constricted air stream of 16-foot diameter.

Changing the angle of attack of the wing from 0° to 3.9° produced little increase of propeller vibratory stress. (See fig. 10.) This result shows that the wake and the downwash behind the wing were affected little by the angle change. Because the presence of the tunnel wall is believed to have limited the downwash, the location of the wake would be expected to change only slightly when the wing angle of attack is increased 3.9°. In accordance with reference 4, a change of 3.9° in the wing angle of attack should produce very little change of the magnitude and the shape of a wake profile.

The simulated split flap on the lower surface of the wing greatly increased the propeller vibratory stress at a frequency of 2n. (See fig. 11.) This increase of stress is attributed to the strengthening and the broadening of the wake. Although the presence of the simulated split flap was also expected to cause a vibration of frequency 1n, no such vibration was detected. With the use of the simulated split flap, however, complete response curves were not obtained for airspeeds higher than 140 miles per hour, because of the dangerously high stresses anticipated.

Figure 12 is a stress curve covering the entire engine-speed range. Although a flatwise vibration having a frequency of 2n was predicted for an engine speed of 1150 rpm (fig. 4), no such vibration was detected, probably because the airspeed at the critical engine speed was only 21 miles per hour. In practice, the velocity of the air with respect to either the wing or pusher propeller would be low for an engine speed of 1150 rpm. During the test the results of which are presented in figure 12, the cement bonding the gages to the blades softened somewhat. The actual magnitudes of the stresses are therefore approximate, but the frequencies are correct and provide a reliable indication that no vibration having a frequency of 2n was present.

Neither a flatwise nor an edgewise vibration having a frequency of 6n was detected (fig. 12). Figure 4 shows that the critical engine speeds for vibrations having a frequency of 6n are 300 rpm, 830 rpm, and 1350 rpm. Of these cases, only the second flatwise vibration

occurring at an engine speed of 1350 rpm would be expected, because the first critical speed is below the operating range and because the airspeed is low for the second critical speed. The fact that no vibration having a frequency of 6n was detected near the blade tips for an airspeed of about 110 miles per hour and an engine speed of 1350 rpm indicates that the third harmonic component of wake excitation was small.

The stress curves of figures 9, 10, and 11 show that the reactionless vibration of frequency 2n excited by the wake is serious. The vibratory stresses considerably exceeded ±2500 pounds per square inch for the shanks. Inasmuch as propellers with more than four blades are also subject to reactionless vibrations at a frequency of 2n, the wake is expected to provide serious excitation for edgewise reactionless vibrations of propellers with four or more blades.

No vibration of the wing was detected that could be attributed to aerodynamic excitation provided by the propeller.

CONCLUSIONS

The results of vibration tests with a wing mounted at thrust-axis level ahead of a four-blade single-rotating propeller to simulate a pusher condition in a constricted air stream of 16-foot diameter indicate the following conclusions:

1. The wake behind the wing supplied serious excitation at a frequency of twice the propeller speed for an edgewise reactionless vibration of the four-blade propeller.

2. The vibratory stress for the reactionless vibration increased considerably with airspeed, but was practically independent of engine brake mean effective pressure for constant airspeeds.

3. The effect of downwash upon the serious reactionless vibration was very small. Changing the angle of attack of the wing from 0° to 3.9° produced no detectable increase of downwash excitation and little increase of wake excitation.

4. A simulated full-span split flap attached to the wing greatly increased the excitation and prohibited the running of tests over the stress peak at airspeeds higher than 140 miles per hour.

5. Agreement between the predicted and the measured value of engine speed for the reactionless vibration was satisfactory.

6. No flatwise reactionless vibration was detected, probably because the airspeeds were low for most of the critical engine speeds and because the harmonic components of wake excitation were small.

Langley Memorial Aeronautical Laboratory,
National Advisory Committee for Aeronautics,
Langley Field, Va..

REFERENCES

1. Kearns, Charles M.: Engine-Airscrew Vibrations. Aircraft Engineering, vol. XIII, no. 150, Aug. 1941, pp. 211-215.

2. Miller, Mason F.: Wind-Tunnel Vibration Tests of Dual-Rotating Propellers. NACA ARR No. 3I11, 1943.

3. Theodorsen, T.: Propeller Vibrations and the Effect of the Centrifugal Force. NACA TN No. 516, 1935.

4. Silverstein, Abe, Katzoff, S., and Bullivant, W. Kenneth: Downwash and Wake behind Plain and Flapped Airfoils. NACA Rep. No. 651, 1939.

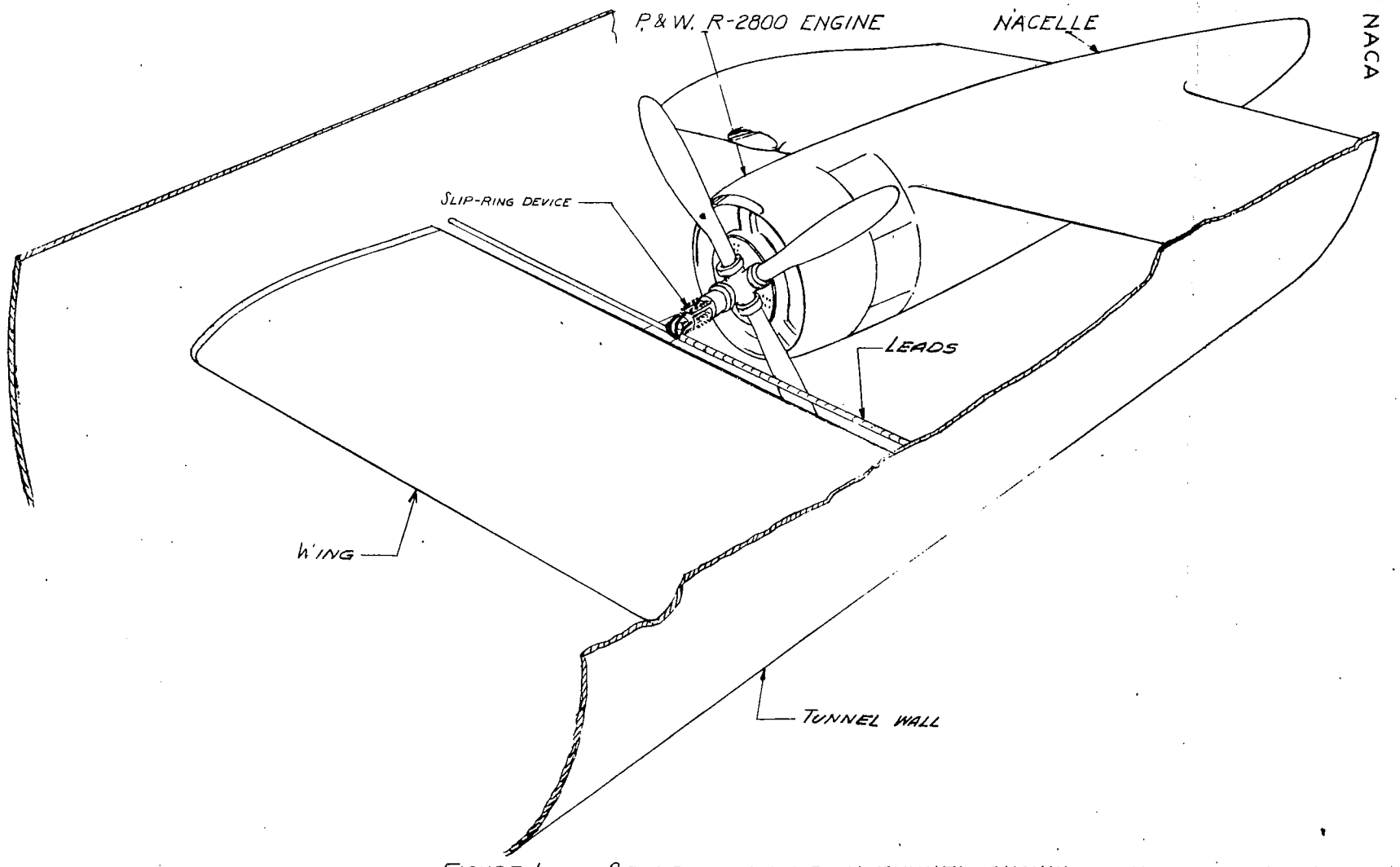

FIGURE 1.— SETUP INSTALLED IN TUNNEL SHOWING WING MOUNTED IN FRONT OF PROPELLER TO SIMULATE PUSHER CONDITIONS.

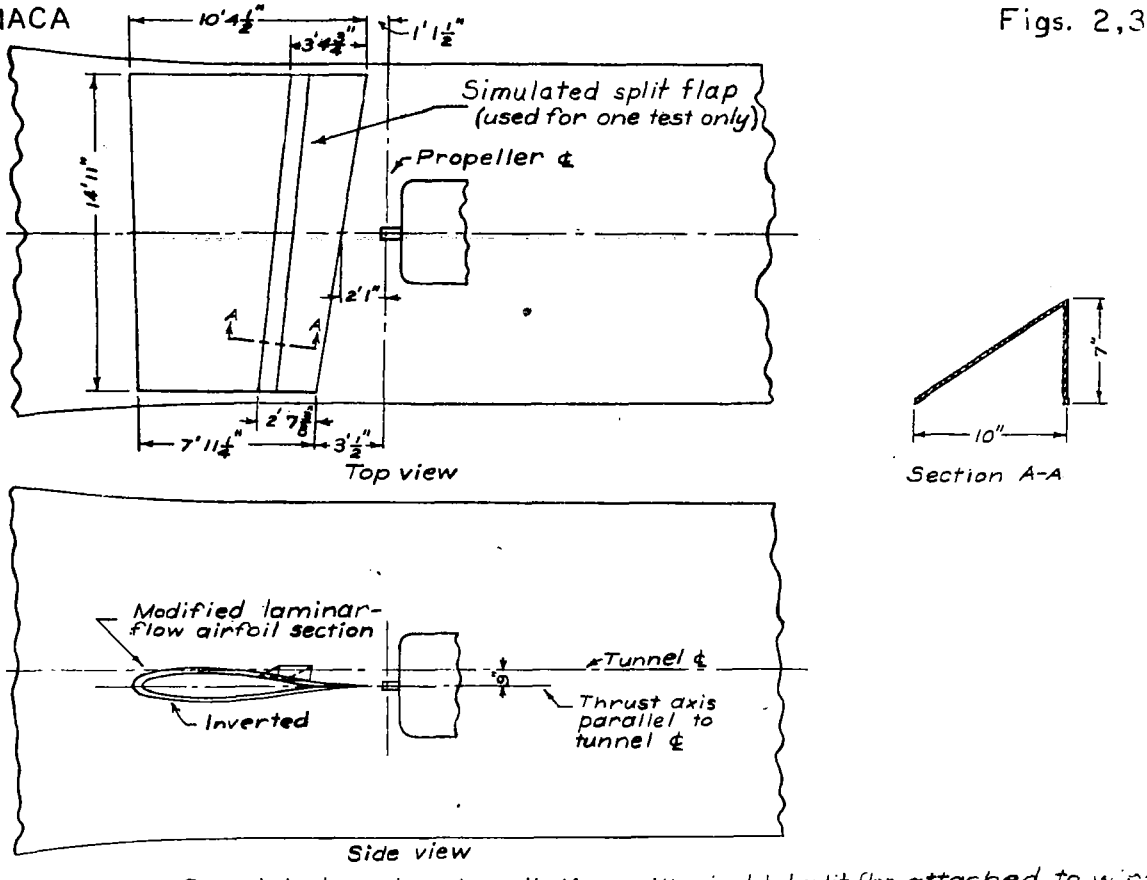

Figure 2.- Simulated pusher installation with simulated split flap attached to wing. α, 0°.

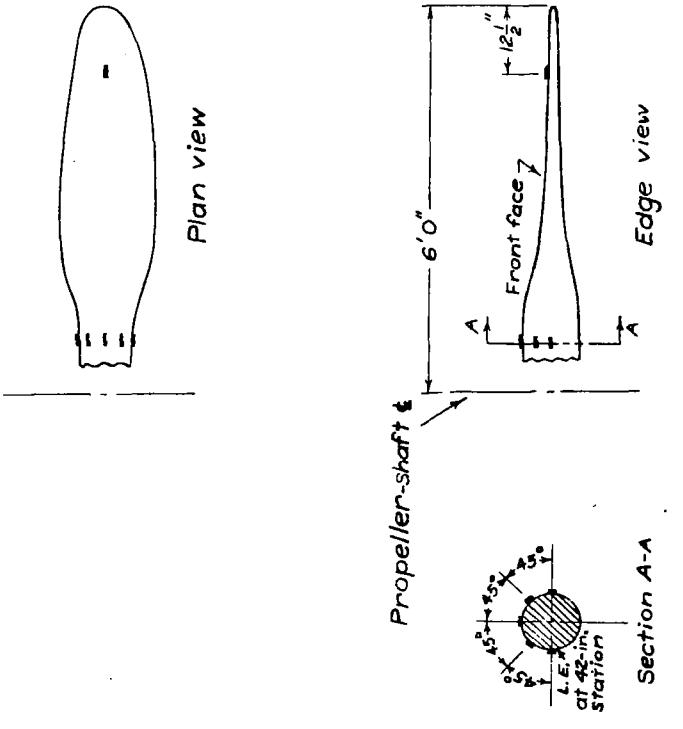

Figure 3.- Location of strain gages on propeller blades.

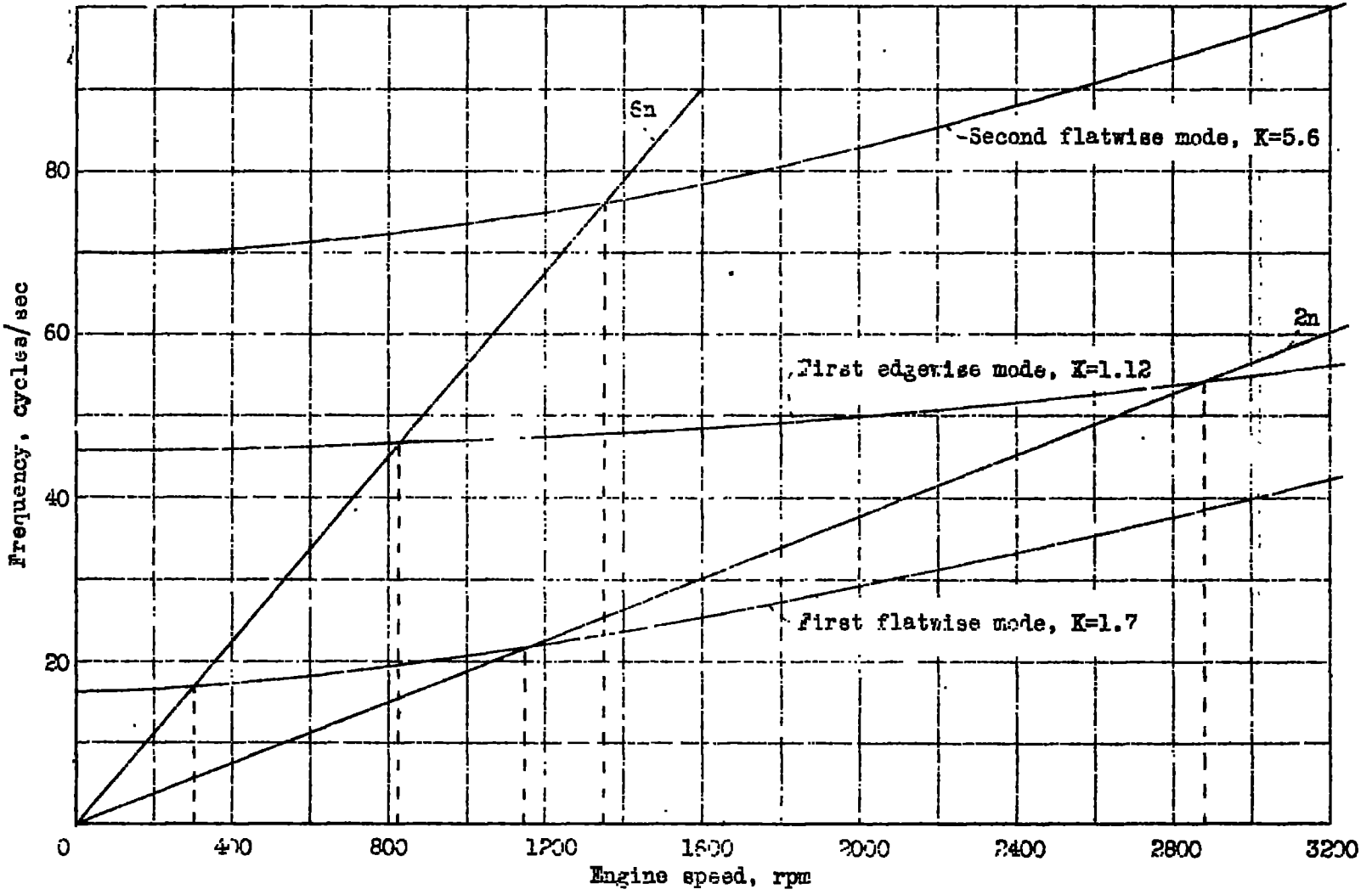

Figure 4.- Engine-speed predictions for reactionless vibrations.

Fig. 5

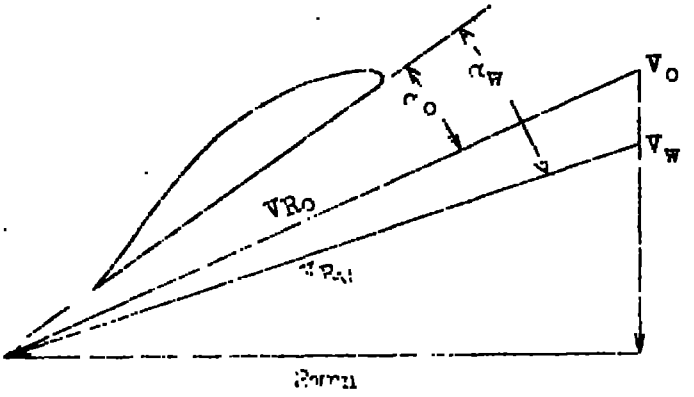

α_o	Angle of attack in free stream
α_w	Angle of attack in wake
r	Station radius
n	Rotational speed
V_o	Forward velocity of air in free stream
V_w	Forward velocity of air in wake
V_{R_o}, V_{R_w}	Respective resultant velocities of a blade element relative to air

Figure 5.- Effect of wake upon the angle of attack and resultant velocity for a blade element.

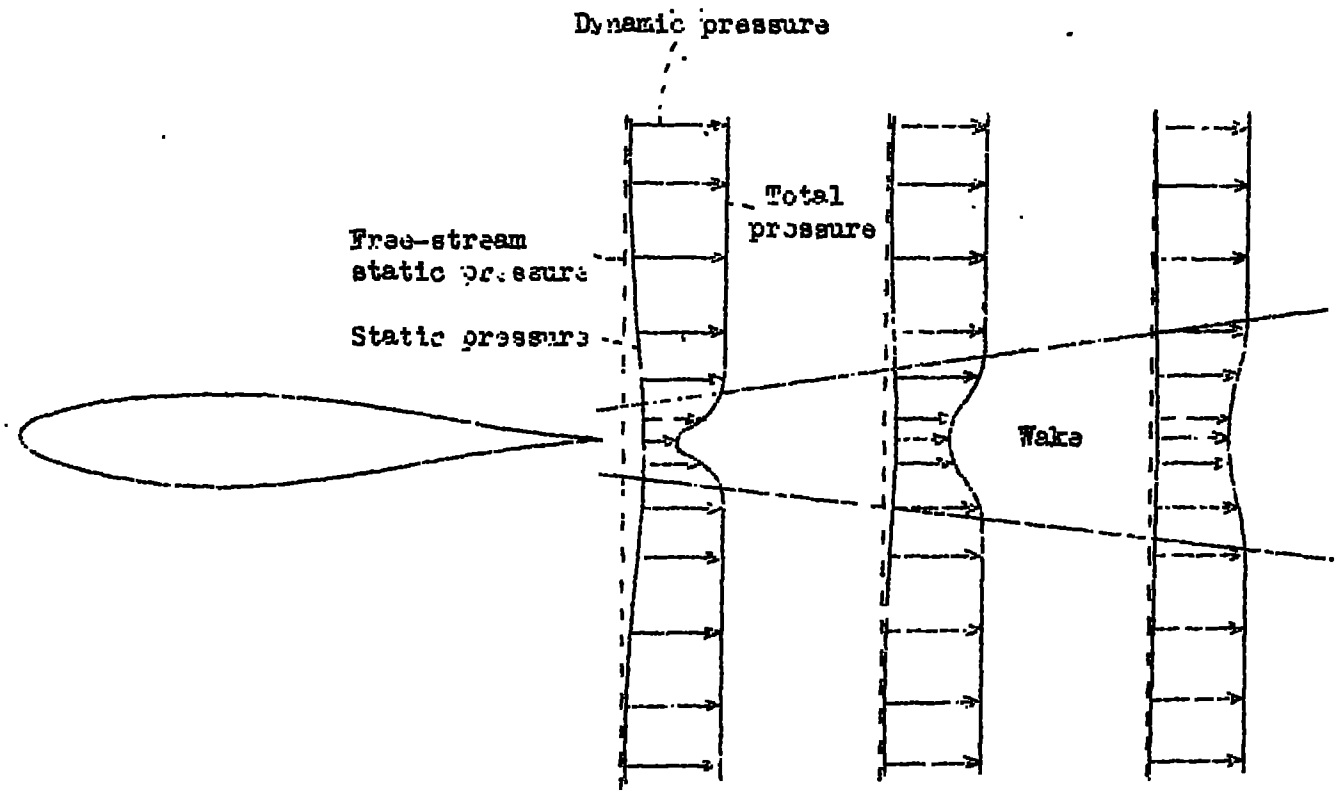

Figure 6.- Total-pressure and static-pressure variations in wake behind an airfoil.

L-327

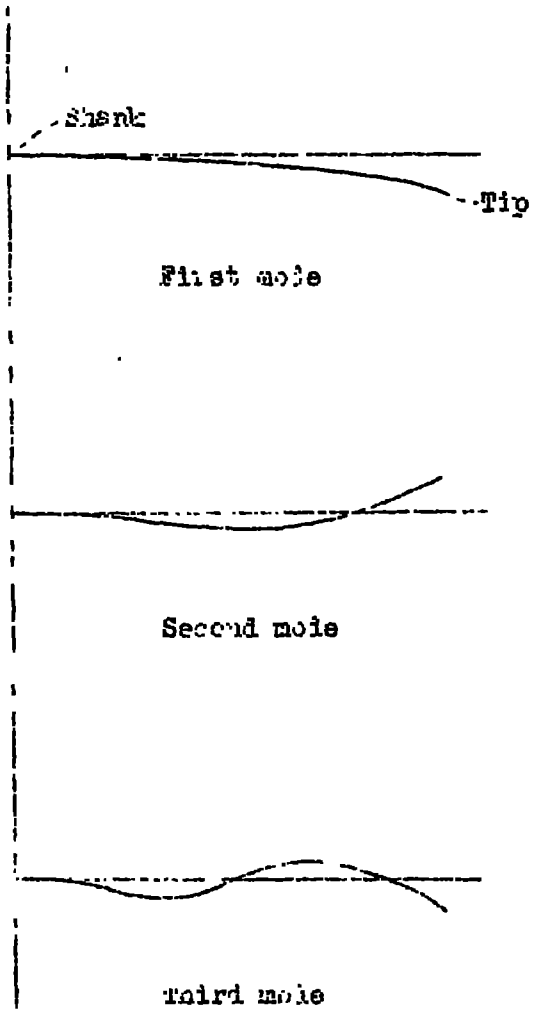

Figure 7.- Mode shapes of vibrating blade.

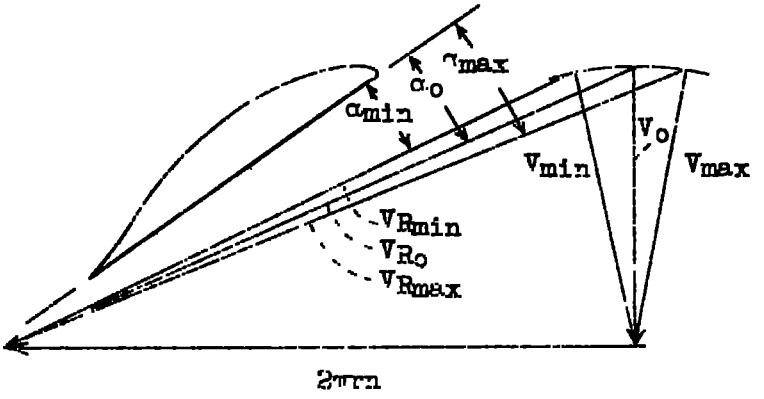

α_o	Angle of attack for no downwash
α_{min}	Minimum angle of attack per revolution with downwash
α_{max}	Maximum angle of attack per revolution with downwash
r	Station radius
n	Rotational speed
V_o, V_{min}, V_{max}	Respective forward velocities of air
$V_{R_o}, V_{R_{min}}, V_{R_{max}}$	Respective resultant velocities of blade element relative to air

Figure 8.- Effect of downwash upon the angle of attack and resultant velocity for a blade element.

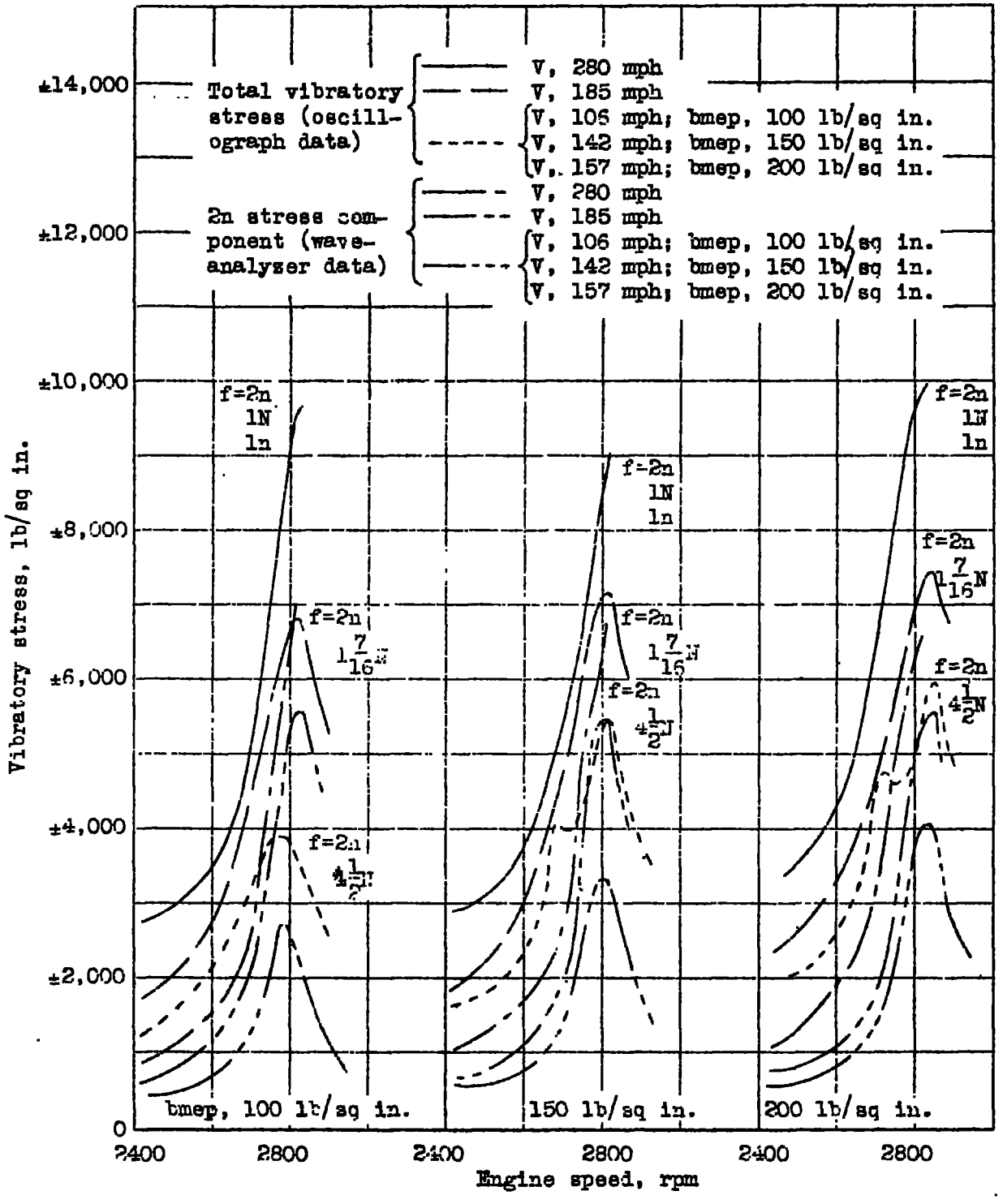

Figure 9.- Effect of airspeed and bmep upon shank stress at leading-edge position. $\alpha = 0^{\circ}$, no simulated split flap on wing.

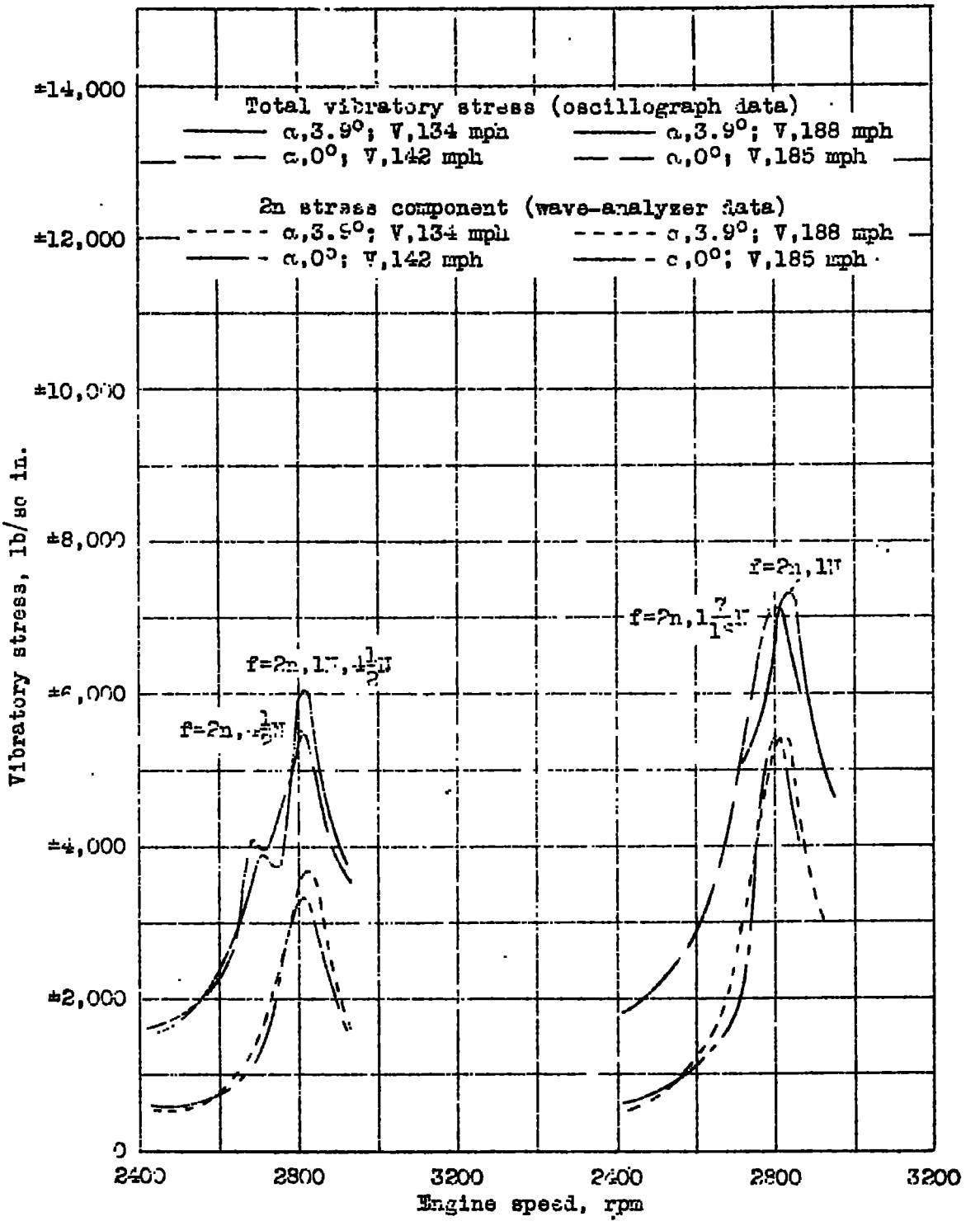

Figure 10.- Effect of wing angle of attack upon shank stress at leading-edge position. Brake mean effective pressure, 150 pounds per square inch.

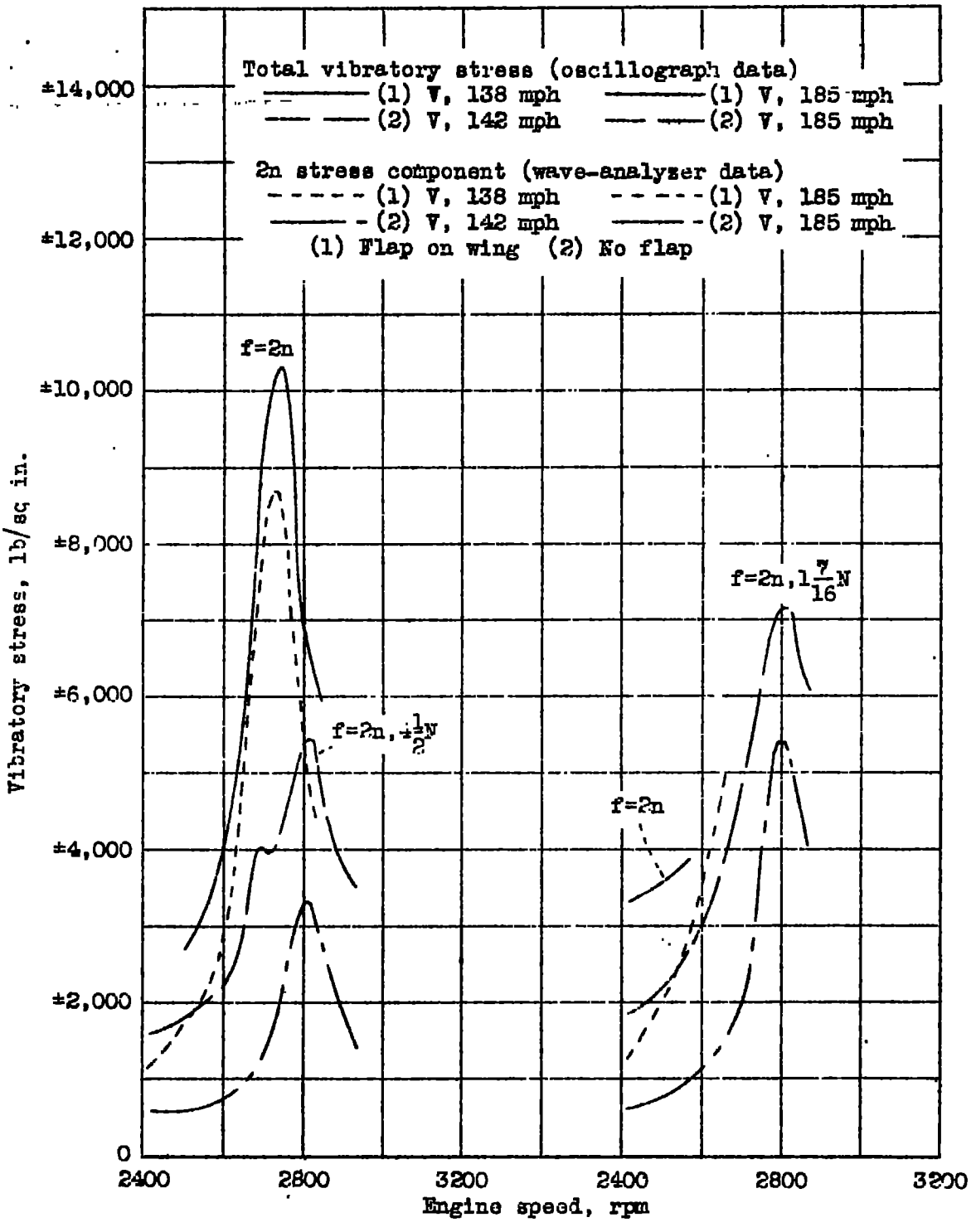

Figure 11.- Effect of simulated split flap upon shank stress at leading-edge position. $\alpha = 0^{\circ}$, bmep = 150 lb/sq in.

L-327

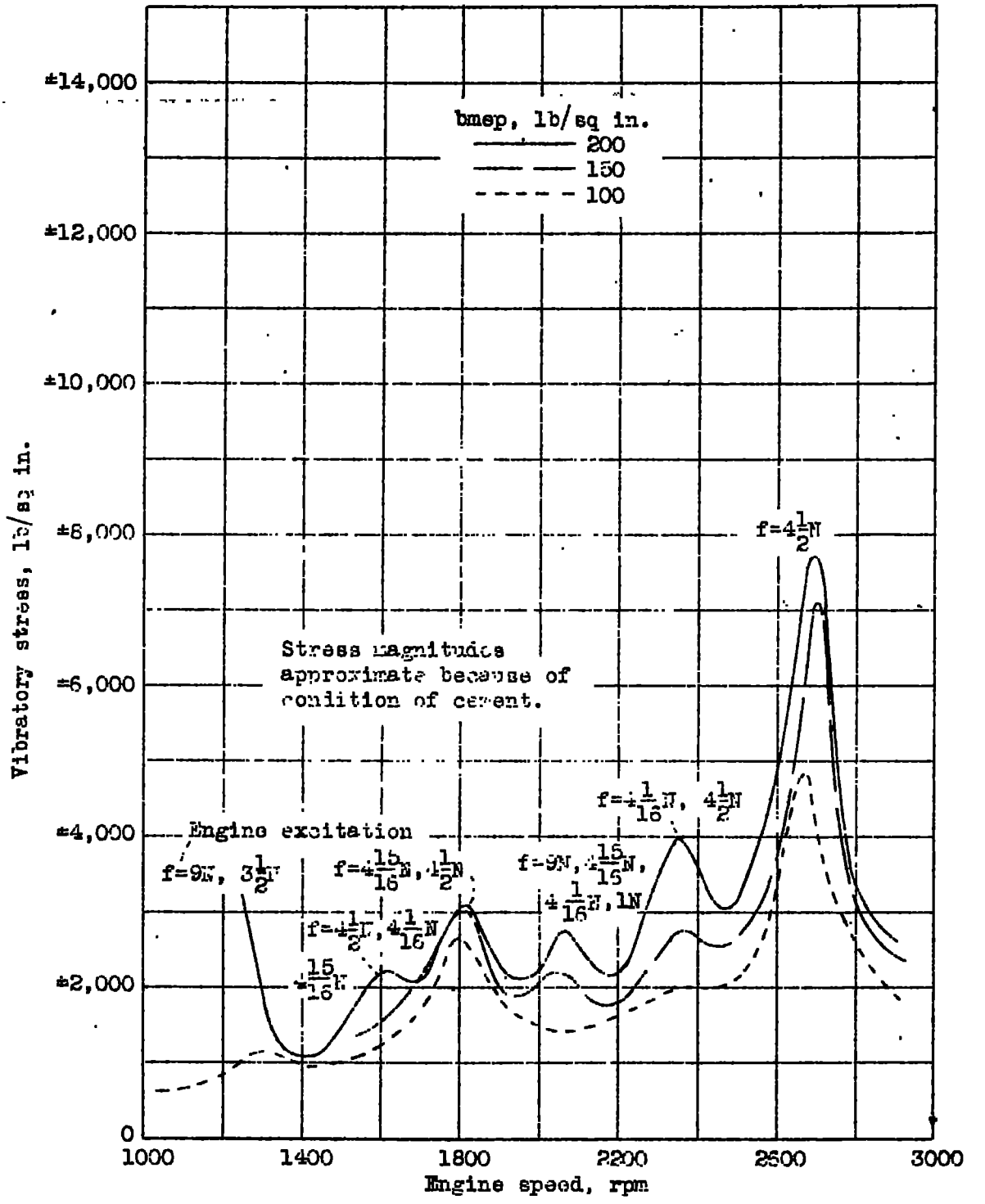

Figure 12.- Summary curves of stress at 12½ inches from tip. $\alpha = 0^\circ$; no simulated split flap on wing; V, below 160 mph.